Low-Level Cloud Development and Diurnal Cycle in southern West Africa during the DACCIWA Field Campaign: Case Study of Kumasi Supersite, Ghana

Jeffrey N. A. Aryee[1], **Leonard K. Amekudzi**[1], **Edmund I. Yamba**[1]

[1]Meteorology and Climate Science Programme, Department of Physics, Kwame Nkrumah University of Science and Technology, Kumasi, Ghana

Key Points:

- Horizontal cold air advection enhanced by NLLJ were dominant LLC development factors
- Impact of LLC evolution and persistence on net radiation flux
- LLC development in SWA characterized by near-steady state net radiation flux, and marginal oscillation about equilibrium in rate of energy storage

Corresponding author: Jeffrey N. A. Aryee, jeff.jay8845@gmail.com

Abstract

The presence, spatial extent and persistence of low-level clouds (LLCs) largely impact on the diurnal surface radiation and energy balance, as well as, the regional climate. Notwithstanding, there is limited understanding on their evolution and processes, particularly in southern West Africa. This paper assesses the development of LLCs and their dominant formative factors, as well as, their relationship with radiation and energy balance. Firstly, ceilometer and radiosondes deployed during the DACCIWA (Dynamics-Aerosol-Chemistry-Cloud Interactions in West Africa) field campaign were used in identifying the LLC. Afterwards, the cloud fraction was employed to characterize different LLC phases. Averagely, break-up, dissipation and build-up of LLC were marked at 0900 GMT, 1200 GMT and 2200 GMT respectively. Moreover, composites of LLC diurnal evolution and their relationship with net radiation, energy storage and surface stability showed that LLCs significantly impact on net radiation flux, by reducing downwelling shortwave radiation. Additionally, LLC onsets were characterized by a near-steady state in net radiation flux, whereas the rate of energy storage within the lower layers marginally oscillated about equilibrium. Finally, with observations from selected intensive observation periods (IOPs), the dominant factors influencing LLC development were evaluated. Horizontal cold air advection, with enhancement by nocturnal low-level jets, was observed to primarily influence the development of LLCs for the study period. Findings of this paper are necessary for improving the understanding of LLC characteristics, formation and interactions with surface properties, particularly over southern West Africa.

1 Introduction

The West African summer months are characterized by copious low-level stratus clouds (LLCs) that persist long into the following day and as such, impact on the surface radiation and energy balance (Knippertz et al., 2011; Schuster et al., 2013), as well as, the regional climate (van der Linden et al., 2015; Bessardon et al., 2018). While these stratiform cloud decks seem to be quite common, they are by no means ubiquitous. However, they have been observed as typical features usually present during the West African monsoon periods. These stratus decks frequently cover an extensive region stretching from the Guinean Coast to about a strectch of 5^o northward of the coast during the night and morning hours (Schrage & Fink, 2012; van der Linden et al., 2015). Although the clouds have been identified to cover a wider spatial domain and to be driven by some atmospheric process, as described in Schrage and Fink (2012); Schuster et al. (2013); Adler et al. (2017), linked with: (i) large-scale advection, (ii) orographic lifting, related to gravity waves, (iii) latent heat release, and (iv) vertical mixing of moisture due to shear-generated turbulence below the nocturnal low-level jet (NLLJ), their interaction with near-surface processes have been under-documented.

Over time, low-level liquid water clouds have been observed to have a large impact on radiative transfer (W. W. Grabowski, 2006; Turner et al., 2007) and consequently, on the diurnal cycle of convection (W. W. Grabowski, 2006; W. Grabowski et al., 2006; Pawlowska et al., 2006; Böing et al., 2012). According to Schuster et al. (2013), the sensitivity of surface radiation balance is coupled more with cloud fraction than surface albedo and temperature in West African intertropical convergence zone. Notwithstanding, there arise complexities to documenting the evolution and dynamics of LLCs, partly due to the difficulty of monitoring these LLCs with satellites due to the relatively small contrasts in warm temperatures between the cloud deck and the underlying surface (Knippertz et al., 2011), as well as, the relating challenges induced by mid- to high clouds (van der Linden et al., 2015).

Presently, there is a limited number of studies on LLC development and dynamics performed over West Africa which are either satellite-based (Knippertz et al., 2011; Schrage & Fink, 2012; Bianca et al., 2018), modelled (Schrage & Fink, 2012; Hannak et al., 2017)

or from observation-based data (Schrage & Fink, 2012; Schuster et al., 2013; Dione et al., 2018; Adler et al., 2019; Babić et al., 2019), with even no evidence-based LLC assessment over Ghana. As part of the core focus of the Dynamics-Aerosol-Chemistry-Cloud Interactions in West Africa (DACCIWA) project to understudy LLC development and its related properties, a two-month intensive field campaign was organized in three supersites (Kumasi, Savè and Ile Ife) and several other ground observing sites across SWA (Knippertz et al., 2015; Flamant et al., 2017; Knippertz et al., 2017; Kalthoff et al., 2018). The DACCIWA Project (spanning June – July, 2016) made use of various atmospheric datasets: near-surface measurements, measurements of dynamics and thermodynamics in the boundary layer and above, measurements of cloud characteristics, aerosol, and precipitation, aircraft measurements, among others. A comprehensive instrumentation list and details on the DACCIWA project is provided in Flamant et al. (2017), with the dataset available on the SEDOO BAOBAB data repository via https://baobab.sedoo.fr/DACCIWA/. The study presented here focuses on assessments from the Kumasi supersite in Ghana, providing detailed information on the dynamics, evolution and formation mechanisms of LLCs in the region.

This paper addresses a two-fold LLC assessment: (i) characterizing LLC and its synergy with surface stability and surface energy balance (hereafter termed as SEB), as well as, (ii) assessing the role of key atmospheric mechanisms to LLC development. The detectable mechanisms influencing LLC development have been assessed using field observations from the Kumasi supersite, for the 2016 summer months in the study region. The paper is structured as follows: Section 2 describes the study area, instrumentation and datasets employed, Section 3 provides results on LLC characterization and its synergy with surface stability and SEB. Section 4, on the other hand, evaluates the dominant forcing factors triggering LLC development. Finally, conclusions are given in Chapter 5.

2 Description of Data Source and Methods

2.1 Data Source

For this study, upper air datasets retrieved predominantly from six-hourly radiosonde launches performed during the DACCIWA field campaign in June - July 2016 from Kumasi, Ghana in southern West Africa were utilised. Vaisala RS-92 sondes were launched during the Intensive Observation Periods (IOPs), spanning from 1800 GMT of the day before IOP until 1800 GMT on IOP day at 6 hr intervals. A total of 15 IOP days are accounted for in Kumasi during the field campaign (Table 1). For non-IOP days, only the 0600 GMT soundings were performed. Towards the end of the project, few one-and-half hour soundings were also launched in Kumasi. As shown in Figure 1 b, the total number of radiosonde launches at each site during the field campaign period have been illustrated in the colorbar, with triangles and circles representing super-site and other radiosonde network stations respectively. Complementing aerosol backscatter profiles were retrieved by the Campbell CS 135 ceilometer at a temporal resolution of 10 s and vertical coverage of 10 km. These provided relevant information on cloud identification and their evolution.

In addition, the flux measurements were retrieved from the flux tower mounted at the supersites, for retrievals of radiation and energy fluxes, with the soil probes providing soil fluxes which include soil temperature, soil moisture and soil heat flux (Kalthoff et al., 2018). An automated weather station (AWS) was again mounted to provide surface profiles and rainfall estimates over the study site.

From Figure 2 a, it is obvious that the entire tropospheric column is characterized by nearly even proportions of moist lower layers and dry upper layers, ranging averagely between 1.5 % and 2.5 % at each 0.5 km altitude separation. The lowest 1 km is observed to be moist throughout the sounding periods, with RH exceeding 70 % generally (Figure 2 b).

Table 1. DACCIWA Intensive Observation Periods (IOPs).

IOP Number	Date (YYYYMMDD)
1	20160617 – 20160618
02	20160620 – 20160621
03	20160625 – 20160626
04	20160628 – 20160629
05	20160630 – 20160701
06	20160702 – 20160703
07	20160704 – 20160705
08	20160707 – 20160708
09	20160710 – 20160711
10	20160713 – 20160714
11	20160717 – 20160718
12	20160720 – 20160721
13	20160723 – 20160724
14	20160726 – 20160727
15	20160729 – 20160730

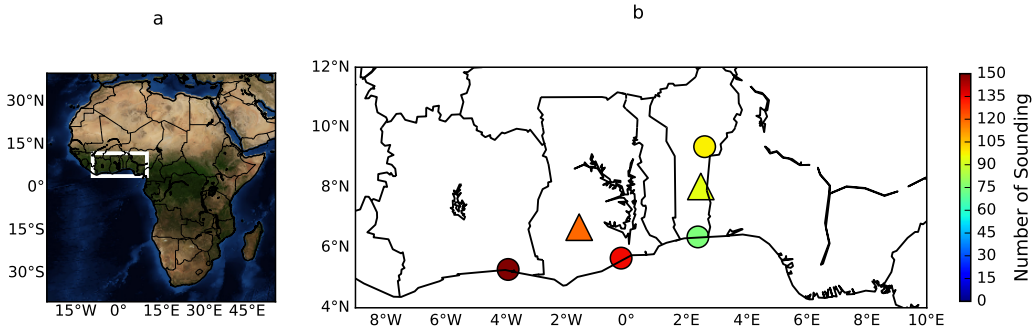

Figure 1. Map of Africa (a) with white bounding box delineating the DACCIWA study domain, and location of radiosonde network (b). The triangles represent the DACCIWA supersites and the circles represent other radiosonde network deployed during the DACCIWA Field Campaign (Kumasi is the inland supersite in Ghana), with the magnitude of soundings for each station provided to match the ranges on the colorbar.

This feature, as expected, occurred mainly because the study region was dominated by southerly to south-westerly winds, which transported more moisture over the region (See wind rose in Figure 2 b). This observation also indicates the dominance of more low-level clouds within the study region during the summer months (Adler et al., 2017; Aryee, Amekudzi, Quansah, et al., 2018; Aryee, Amekudzi, Atiah, et al., 2018; Baidu et al., 2017; Bessardon et al., 2018).

2.2 Assessment Method

2.2.1 LLC Detection from Radiosondes

Radiosonde profiles were used to validate low-level stratiform clouds detected from the ceilometer aerosol backscatter. Radiosonde profiles, during ascent, provide substantial *in situ* upper air observations, and thus serve as reliable information for validating the

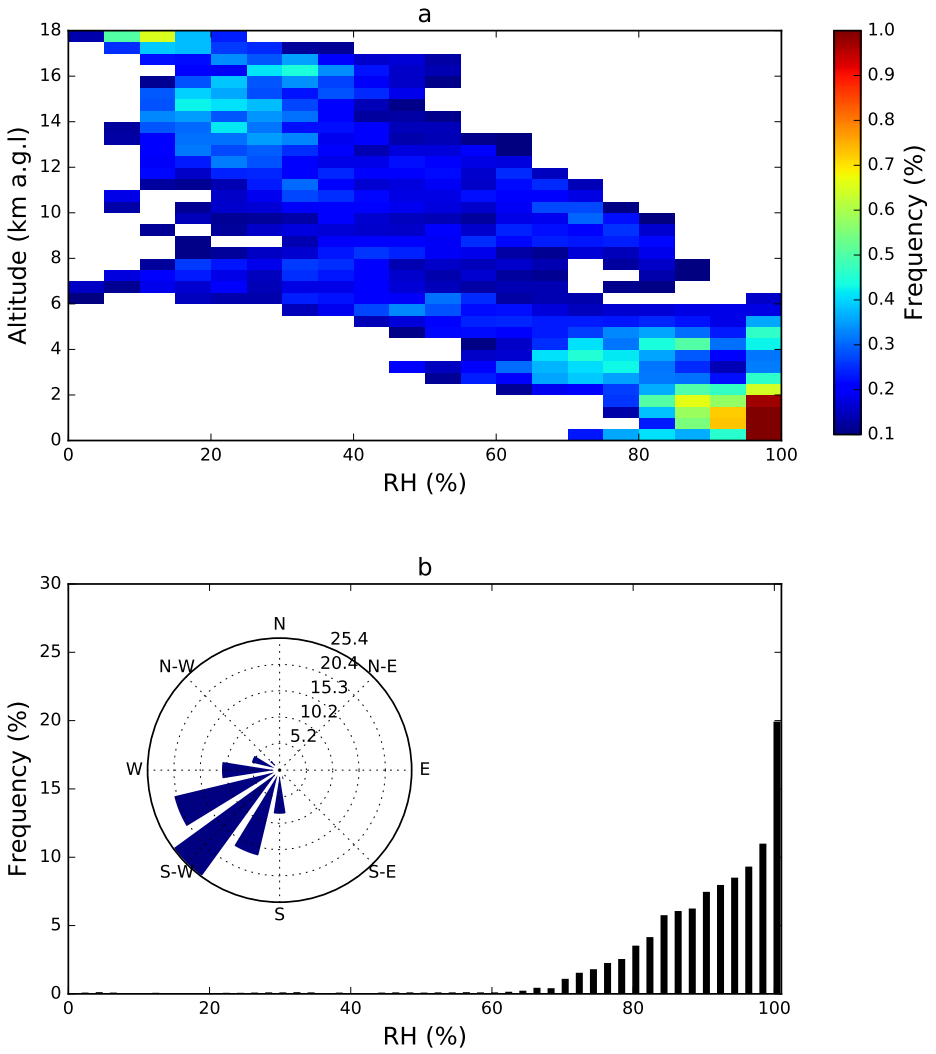

Figure 2. Frequency distributions of RH, from radiosonde data, at (a) all vertical levels and (b) within the lowest 1 km in Kumasi. Rose map in **b** represent the dominant wind direction within the 1 km lower atmospheric region.

rather remotely-sensed ceilometer profiles. Possible sources of error in upper air sounding by radiosonde are linked to spatial drifts of the sonde caused by sheering winds during vertical ascent. The radiosonde therefore has varying profile locations at varying times and altitude. Nonetheless, the assumption largely made here is that, there is just a marginal drift and properties at higher altitudes are mostly stratified and thus render error margins to be relatively minimal. As convention for the sondes to be near the tropopause at the nominal time, the radiosondes were launched about 30 minutes or less before the synoptic hour. The atmospheric profiles deduced by the radiosondes were vertically bin-averaged in steps of 50 m to allow for outlier removals while yet maintaining the atmospheric signature. To identify cloud bases, the Wang and Rossow (1995) approach [also detailed in Kalthoff et al. (2018)] was employed. Since clouds form at super-saturated levels, the lowest level of a vertical extent spanning more than 100 m depth where relative humidity was beyond 99 % was identified as the cloud base.

2.2.2 LLC Detection from ceilometer

, the Campbell CS135 ceilometer used for this study is monostatic (transmission and reception are at same location), thereby providing upper air information from one point of the atmosphere as average for the spatial domain of observation. The ceilometer has vertical coverage of maximum 10 km in clear weather conditions, and an observation frequency of 10 seconds.

were deduced from the ceilometer's aerosol backscatter profile by setting a threshold of $0.15\,\mathrm{m}^{-1}\mathrm{sr}^{-1}$ (optimal for distinguishing backscatter information of tiny atmospheric particulate matter from clouds) beyond which the LLC is defined. Considering the location of the observatory which was not farther from the roadside, the criteria was tested for profiles beyond 100 m in order to avoid identifying potential vehicular aerosols among other surface aerosols as LLC base. Additionally, the identified LLC must extend beyond 100 m, before considered as such. This was in order to eliminate the erroneous identification of aerosols (dust, etc.) as LLCs.

2.3 Intercomparison of Radiosonde- and Ceilometer- Deduced LLCs

In order to compare the deduced LLC base from the radiosonde and ceilometer, the sounding profiles between 2100 GMT and 1200 GMT were used since they match the period for formation, break-up and dissipation of LLCs. In all, 44 sounding profiles with LLCs present were identified from the Kumasi supersite.

a measure or representativeness, the pearson's correlation co-efficient and bias was employed to assess how well LLC deduced by the ceilometer match that of the radiosonde. In all, LLCs by both methods were matched more than half the number of soundings, which is a good representation. A bias of 11%, showing an underestimation of radiosonde-deduced LLCs by the ceilometer is however expected, due to (i) the differences in their measuring principles and (ii) the observed region, especially the drift in radiosonde ascent due to the vertical wind shear.

sample inter-comparison of radiosonde-deduced and ceilometer-deduced cloud bases estimated from 1st to 3rd July has been shown in the Appendix, as well as the overall correlation co-efficient and bias.

3 Results

3.1 Characteristic Phases of Low-level Cloud Development

LLCs, as observed in Figure 3, persist throughout the nighttime hours till approximately 1200 GMT over the supersite, having thickness of approximately 200 m. Before sunrise, the LLC base oscillated between 150 and 250 m a.g.l, showing some general reduction in heights from midnight to morning, which results from nocturnal low-level cooling. These findings support the role of NLLJs in transporting either moisture or cool air onto the surface, thereby cooling the lower layers and rendering them moist; a necessary condition for the presence of clouds in the lowest regions.

About an hour after sunrise, LLCs were observed to gradually rise till maximum heights were attained between 1100 GMT and 1230 GMT. However, on very cloudy days, these stratiform clouds persisted at low levels - even beyond midday - thus limiting downwelling shortwave radiation flux onto the surface.

Afterwards, the number of detected LLCs per every 15 minutes were binned as percentages of the maximum permissible LLCs that can be detected in each time interval. Hence, the cloud fraction was computed as the number of identified LLC bases divided by the maximum permissible cloud bases (15) and then multiplied by 100. On average, the night-

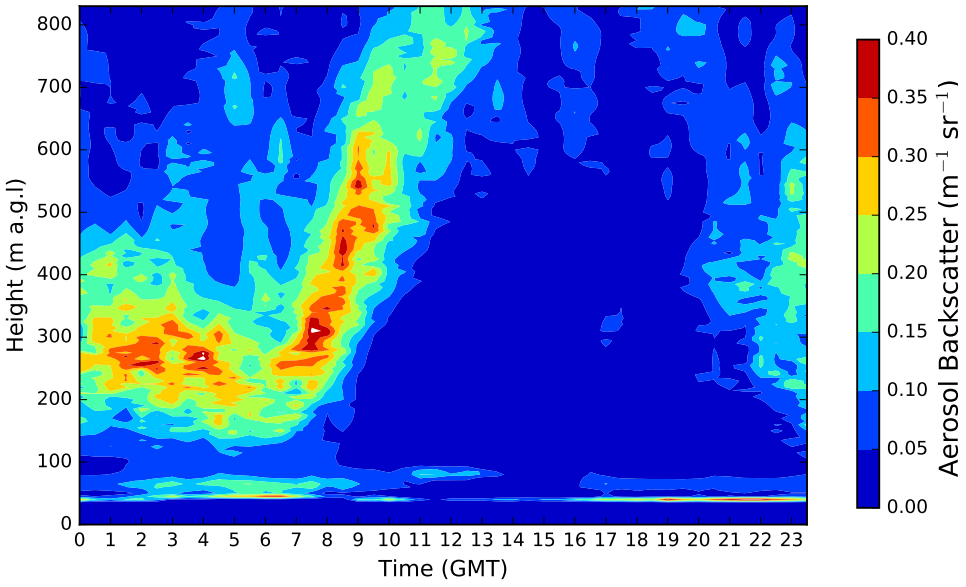

Figure 3. Composites of mean vertical aerosol backscatter from the Kumasi supersite.

time periods were marked with extensive cloud cover (CF $\approx$ 100 %; see Figure 4) which were mostly formed at 2230 GMT and persisted at low levels till after sunrise hour when they were vertically advected. Approximately two and half hours after sunrise (0900 GMT), with the onsets of downwelling shortwave radiation, the low-level stratiform clouds were observed to break-up into cumuliform clouds (marked by CF $\leq$ 95 %).

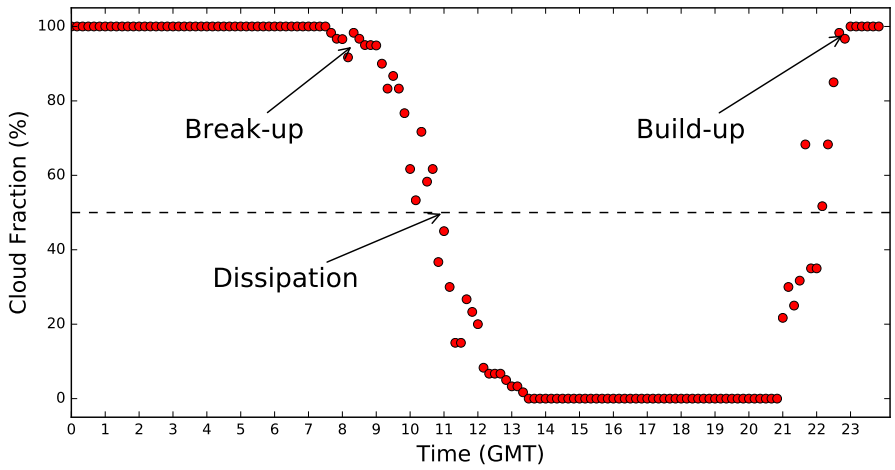

Figure 4. Characteristic phases of LLC development deduced from the cloud fraction (CF).

Between the periods of 1100 GMT and 1230 GMT, LLCs were observed to dissipate; mostly advecting vertically into mid-atmospheric layers, which are linked to heightened surface

heating. To identify LLC dissipation, a threshold of 50 % (CF $\geq$ 50 %) was set. This threshold helps to identify the bins in which approximately half of the cloud layer is absent in a 15-minute interval, and observed to last for some recurrent time. Moreover, when LLC per bin was observed to be greater than 95 % (CF $\geq$ 95 %) - beyond sunset hours - those periods where marked as the build-up (onsets) of LLCs. The diurnal cycle is thus repeated.

3.2 Relationship between Surface Stability and Low-level Cloud Development

The onsets and absence of downwelling shortwave radiation (sunrise and sunset) have large impacts on the diurnal surface stability evolution. We attempt at identifying the relationship between the surface stability profiles and the presence and location of LLCs. Monin-Obukhov length ratio was used in assessing the surface stability profiles.

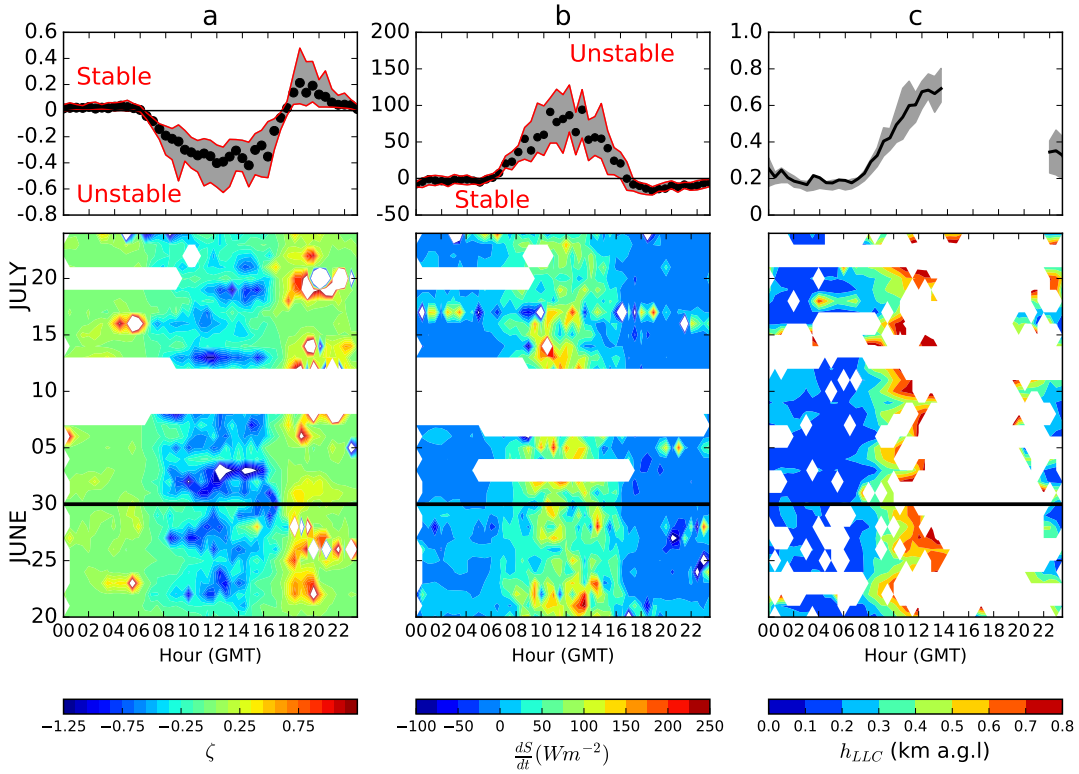

Figure 5. Diurnal evolution of (a) surface stability, (b) rate of energy storage in the lower layers and (c) LLC altitude. The mean profiles are shown above as points, bounded by the grey region representing 25^{th} and 75^{th} percentiles. Diurnal evolution for individual days during the observation period are also shown below.

Figure 5 captures the diurnal evolution of surface stability (left), energy storage within the lower layers (middle) and LLC (right). Nighttime hours are characterized by low energy storage values and stable lower layers (ζ >0) which mostly rendered the LLCs at lowest altitudes (mostly below 0.3 km). Sunrise hours triggered positive changes in energy storage within the lower layers and generally altered surface stability from stable to unstable phases (ζ <0), with increased LLC heights. Increasing diurnal trends in energy storage within the lower layers correspond to changes in surface stability and LLC location. Similar to earlier results, LLCs were observed to form mostly after 2100 GMT,

when the surface of the study location had returned to a near-neutral state, with energy storage also returned to a near-equilibrium state.

4 Evaluation: On Dominant Forcing Factors Triggering LLC Development

To allow for comprehensive assessment of the relationship between LLC characteristics, PBL evolution and radiation and energy balance, 12 IOPs were selected as case studies (see Table 1) - comprising of IOPs 2 to 13. For all IOP days, the preceding day's observations were also included to allow for two complete diurnal cycles of the surface and atmosphere variables. Out of all 15 IOPs during the DACCIWA campaign, IOPs 1, 14 and 15 were rejected due to missing data, associated with technical and operational challenges.

4.1 Interactions of LLC development with radiation and energy balance

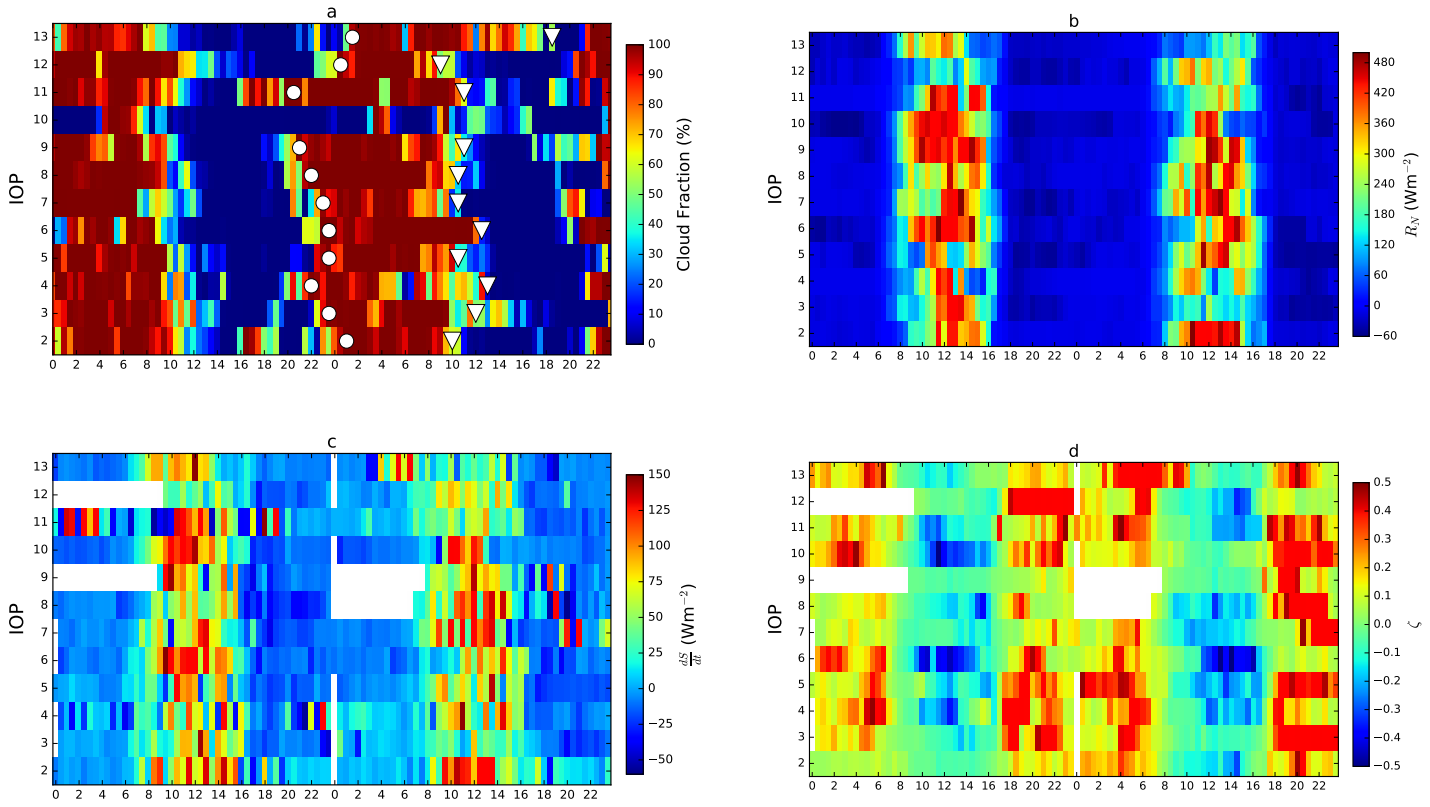

Figure 6. Diurnal evolution of (a) LLC fraction, (b) net radiation, (c) rate of energy storage and (d) surface stability from Kumasi supersite during the DACCIWA IOPs. White circles indicate onsets of LLC and white triangles show the LLC dissipations.

Figure 6 highlights the diurnal evolution of LLC fraction, net radiation, rate of energy storage and surface stability in Kumasi, from the 12 selected IOPs. Similar to Figure 4, LLCs mostly existed from the evening of the preceding day till early afternoon of the IOP; except IOP 10 which was marked by almost a cloudless lower atmosphere (cloud fraction predominantly less than 50 %), as well as, IOPs 4 and 12, which were also marked by early reductions in cloud fraction. The influence of these cloud properties on evolu-

Table 2. Cloud cover information (low cloud, mid-altitude cloud, high cloud) from the Ghana Meteorological Agency (GMet) manned weather stations at Kumasi Airport for selected IOPs. x denotes no observable cloud type.

IOP Number	00	03	06	09	12	15	18	21
06	5,x,x	5,x,x	5,3,x	5,3,x	8,3,x	2,3,0	2,3,0	5,3,2
10	5,3,x	5,3,0	5,4,x	5,3,x	8,3,x	8,3,x	5,3,x	0,3,x
11	5,x,x	5,x,x	5,x,x	5,3,x	8,3,x	2,3,0	2,3,0	0,3,0
13	5,3,0	5,2,x	5,7,x	5,7,x	8,3,x	8,3,x	8,3,x	0,3,0

tion of the radiation and energy balance, as well as, the surface stability profile is further provided in Figure 6.

The persistence of LLCs into early afternoon hours have been observed to modify the downwelling shortwave radiation (Knippertz et al., 2011; Schuster et al., 2013), which further impacts on the diurnal net radiation profile. For example, extensive LLC structures on IOP 3 reduced the net radiation flux at early daytime hours by approximately $100\,\mathrm{W\,m^{-2}}$. Similar observations were again made from IOP 13, where LLCs persisted till late afternoon hours, thus, reducing R_N by similar magnitude.

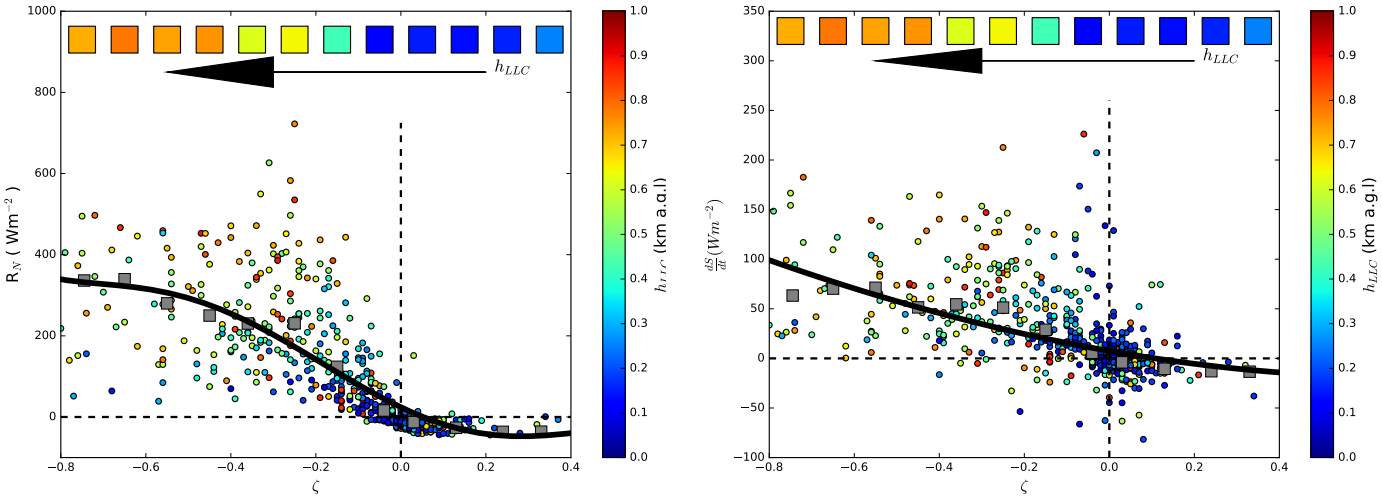

Figure 7. Development of LLC in response to changes in (a) ζ and R_N, as well as, (b) ζ and $\frac{dS}{dt}$.

Despite the minimal amounts of low-level cloud decks on IOP 10, the magnitude of R_N was relatively reduced from sunrise, which is likely attributable to the radiative forcing of mid-altitude clouds, or possibly, feedback of the dry air intrusions that emanated from the subsidence area in the equatorial zone or the southern hemisphere by the southern anticyclonic vortex, as discussed in (Knippertz et al., 2017). These, however, can not be fully substantiated from the ceilometer profiles for the day. Cloud observations from the manned synoptic weather station at Kumasi airport however reports on the presence of low to mid-altitude clouds throughout the day (see Table 2), which obviously, the vertical limit set for the ceilometer profiles in detecting LLCs were unable to locate.

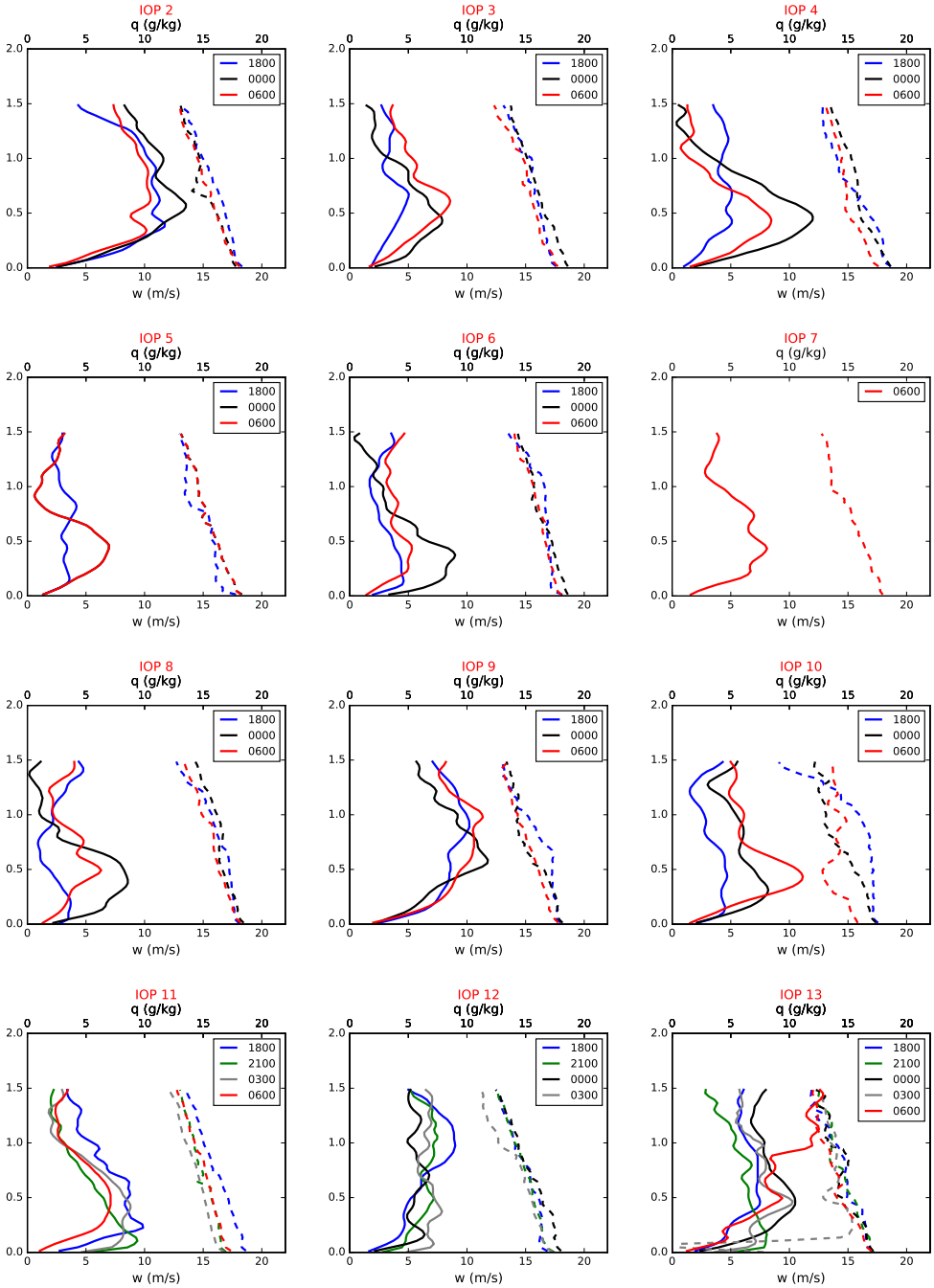

Figure 8. Vertical profiles of wind speed (thick line) and mixing ratio (dashed line) from soundings performed in Kumasi between IOPs 2 and 13.

LLC radiative forcing also reflect substantially in modifications in the rate of energy storage within the lower layers (see Figure 6 c). From Figure 6 d, the surface layer at nighttime, corresponding to hours of maximum cloud fraction, is stable. Thereafter, the stability profiles evolve into more unstable phases after sunrise, due to convective onsets, with these hours also marked by reductions in the cloud fraction; depicting the break-up phase of stratus into stratocumulus and cumulus clouds. Cloud layers again form approximately four hours after sunset, marked mostly by very stable surfaces.

The interactions between the diurnal evolutions of LLC, R_N and $\frac{dS}{dt}$ are as illustrated in Figure 7. Periods of surface stability ($\zeta > 0$) were equally marked by R_N less or equal to 0. Increases in R_N further triggered changes in the surface stability profiles (from stable to unstable phases), and similar interaction was also observed between ζ and $\frac{dS}{dt}$. Generally, the interactions between the ζ and R_N, as well as, ζ and $\frac{dS}{dt}$ were found to be related by a polynomial function, as illustrated in Figure 7 (equations on the plot area). Moreover, transition from stable to unstable regions were also marked by increases in the height of the LLC base, with accompanying decrease in low-level cloud fraction.

To understand the atmospheric mechanisms that aid the formation of LLCs in the region, the wind speed and mixing ratio profiles were assessed, as shown in Figure 8, since they are key indicators on moisture transport and subsequently provide highlight on their respective roles in LLC formation (Lothon et al., 2008). For this part, only the upper air soundings made between the formation and break-up times of LLCs were studied. Deepening of the stable nocturnal layer, due largely to radiative cooling, intensifies the NLLJ and shifts them towards higher altitudes (Madougou et al., 2012). Due to their speeds - although NLLJs in the monsoon season have lower speeds than the dry/Harmattan season (Lothon et al., 2008) - and direction of propagation, which is predominantly southerly to south-westerly, the characteristic NLLJs, similar to observations in (Schuster et al., 2013), advect moisture onto the study domain. Although drying ($\leq 1.5\,\mathrm{g/kg}$) is observed in most IOP nights, the mixing ratio magnitudes beneath the NLLJ core indicate significant amount of water vapour in the lower atmosphere. Convection arising after sunrise leads to a rapid mixing between the surface momentum and the LLJ shear momentum which tends to mix the moisture within the PBL (Madougou et al., 2012; Schepanski et al., 2015).
An exceptional case of the influence of NLLJ on mixing ratio profile is identified on IOP 10, which was within the vortex phase of the Monsoon season. Although the NLLJ was fully formed between 0000 GMT and 0600 GMT, moisture profiles declined largely at the location of the NLLJ, by approximately $3.5\,\mathrm{g\ kg^{-1}}$. These are possibly linked to the dry air intrusions that emanated over the study region from the subsidence area in the equatorial zone or the southern hemisphere by the southern anticyclonic vortex (Knippertz et al., 2017).

4.2 Influence of NLLJ and low-level stability on LLC development

In Figure 9, distribution of the cloud fractions at 3 threshold values has been provided. For brevity, cloud fraction greater or equal to 95% (mostly representing extensive, stratiform cloud deck) is denoted by CF1 and those above 50 % but below 95 % are denoted by CF2. CF3, as used here, represents no low cloud (below 25 % cloud fraction). The nighttime hours were dominated by CF1, as seen by at least 50 % of the observations within each 30 minute interval and relatively few CF2 (see Figure 9 a). However, in the post-sunrise periods (after 0600 UTC), CF2 increased steadily (by approximately 25 %) whereas CF1 reduced marginally and throughout the day until LLC onsets again at night. Reductions of CF1 and accompanying increase in the magnitude of CF2 within the LLC break-up and dissipation periods confirm the observations in Figure 4, that the nocturnal low-level stratus decks are fragmented during this period. The fragmentation, from this study, are linked with the solar heating after sunrise hour and the subsequent turbulence generated, which mixes properties (surface momentum and the LLJ shear mo-

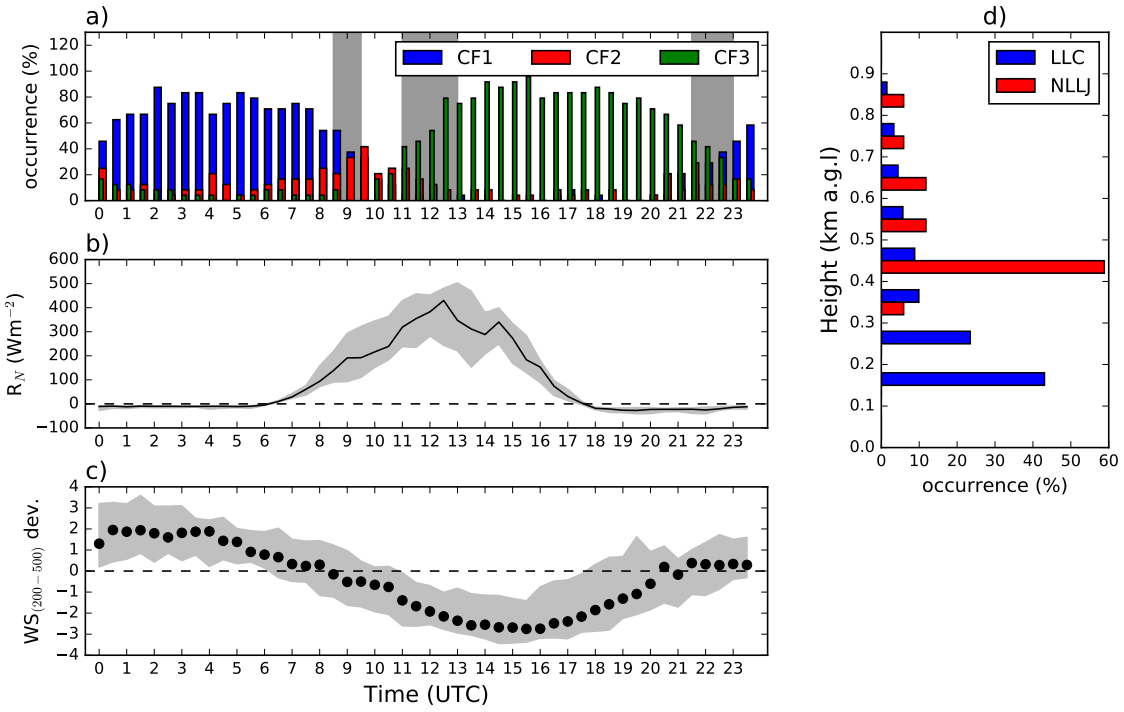

Figure 9. Distribution of (a) cloud fraction, (b) net radiation, (c) diurnal deviation of wind speed located in the NLLJ region and (d) height a.g.l of the LLC base (blue) and NLLJ (red). Gray-shaded regions in **a** mark the LLC break-up, dissipation and build-up/onset times respectively. CF1 denotes cloud fraction greater or equal to 95 %, CF2 denotes cloud fraction above 50 % but below 95 % and CF3 represents cloudless periods (cloud fraction < 25 %). Gray-filled region in **b** and **c** also represents the 25^{th} and 75^{th} percentiles. Wind speeds in **c** are from the deployed SODAR at the field site.

mentum) within the PBL (Lothon et al., 2008), and as such, impacts on the cloud structures.

To characterize the NLLJs, the median of winds between the 200 – 500 m a.g.l layer (denoting the NLLJ region) at respective times were divided by the diurnal average wind speed within the jet region (see Figure 9 b). By this, temporal regimes where NLLJs were present were marked by positive deviations, and temporal regimes dominated by by mixing were marked by negative deviations. NLLJs were observed to be stronger between 0000 GMT and 0500 GMT, with periods between 0030 GMT and 0800 GMT dominated by extensive, stratiform cloud decks (CF1).

Again, as shown in Figure 9 b, within the post-sunrise hours, generation of convective thermals within the PBL mixed and overturned the winds within its layer. As a result, NLLJs are depleted as evidenced by the transition from positive $\mathrm{WS}_{(200-500)}$ to negative $\mathrm{WS}_{(200-500)}$. The periods of total depletion of the NLLJs (approximately 0900 GMT), were also marked by break-up of these stratus clouds (see Figure 9 a; increase in distribution of CF2 and accompanying decrease in CF1). Moreover, the break-up to dissipation phase of LLCs, as expected, were dominated by rapid turbulent mixing (Figure 9 b), drastically reducing cloud fraction (maximum CF3 proportion).

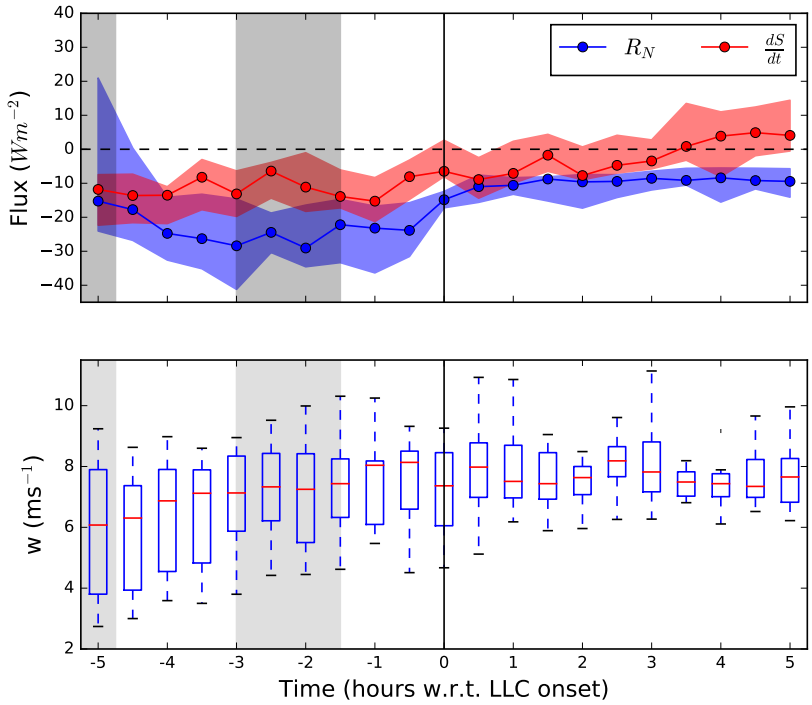

Figure 10. Median of (a) R_N and $\frac{dS}{dt}$, and (b) wind speed with respect to LLC onsets. Filled regions in the upper panel and boxes in the lower panel represent the 25^{th} and 75^{th} percentiles. Grey-shaded region on the left denotes the sunset hours and shaded-region on right marks earliest NLLJ detection

Figure 9 d captures the altitudes of LLC and NLLJ. The altitudes of NLLJs were detected from radiosonde launches at the synoptic hours of the stated periods in Table 1. The NLLJs

were mostly located at 0.4 – 0.5 km a.g.l, totalling approximately 60 % of the entire occurrence. Also, LLCs were located predominantly beneath the NLLJs, which totalled about 80 % of the entire LLCs detected. These information corroborate findings of (Knippertz et al., 2011; Schrage & Fink, 2012; Schuster et al., 2013), that the NLLJ contributes to the formation of LLCs in SWA. However, the shear-generated turbulence in the lower layers were found to be limited by statically stable regions existing between the turbulence region and the cloud base.

Figure 10 details both the pre-LLC and post-LLC radiation and energy storage fluxes within the lower layers. Lower atmospheres, after sunsets, are dominated by radiational cooling as observed in Figure 10 a. Upwelling longwave radiation, coupled with soil heat flux emanating from the surface tends to maintain the energy balance. The onsets of LLCs were also marked by a near-steady state in the net radiation flux, whereas the rate of energy storage within the lower layers marginally oscillated about equilibrium. This pattern continues until convective onsets at sunrise, when downwelling shortwave radiation produces thermal currents that destabilize air in the lower atmospheric column, which results in increase in the PBLH and also forces the base of LLCs to vertically rise.

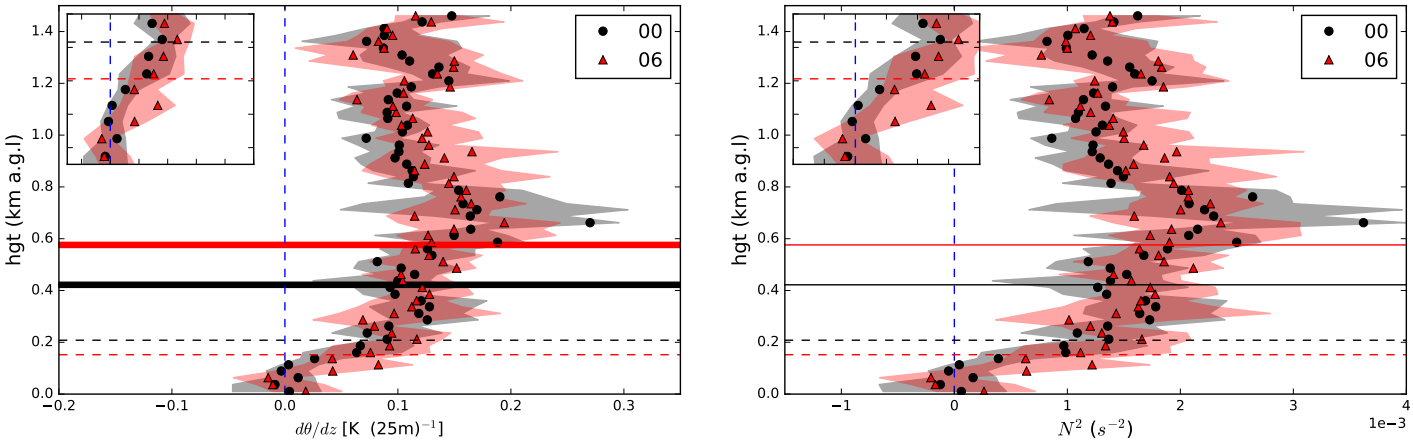

Figure 11. Median of static stability (left) and square of Brunt-Väisälä frequency (right) deduced from radiosoundigs in Kumasi at 0000 GMT (black) and 0600 GMT (red). The filled regions represent the 25^{th} and 75^{th} percentiles. Thick horizontal lines mark the locations of NLLJ and dashed horizontal lines mark the LLC base at the respective times. Inset in top-left shows the profiles below the LLCs. Blue, dashed vertical delineates the separation of statically unstable regime (left) from statically stable regime (right).

Mechanical turbulence driven by the wind shear underneath the NLLJ has been proposed as an important factor for stratus formation in West Africa (Knippertz et al., 2011; Schrage & Fink, 2012). Hence, the influence of the NLLJ on stability structure of the lower atmosphere, especially beneath the jet, was also assessed (see Figure B2 a). This allowed for identification of unstable and stable lower layers, where there is vertical mixing of moisture, and where the mixing is suppressed, respectively. With the high sampling frequency of radiosonde in Kumasi, a 25 m vertical resolution was adopted to assess the stability of the layer at smaller intervals. The 25 m interval has the ability to maintain the profile signatures, while also capturing the intermittent turbulent structures within the lowest layers. Statically unstable regions were identified beneath the LLC alright, sim-

ilar to earlier observations (Schrage & Fink, 2012; Schuster et al., 2013), however, they were capped by statically stable regions of same vertical extent as the unstable region. Such episodes were observed on more than half of the IOP days.

Air parcels are likely to be intermittently turbulent within the marginally, unstable low regions. However, their influence on the LLC development and its persistence seem to be restricted by the statically stable region above it, which likely minimize any significant vertical mixing or overturning of properties between the unstable surface regions and the LLC. These observations are corroborated by the squared of Brunt-Väisälä frequency estimates, shown in Figure B2 b. Buoyant lower layers are suppressed by the statically stable regions lying above them, and hence, may have only marginal influence on the LLC development.

As evidenced in the insets of Figures B2 a and B2 b, the turbulent region is rather lowered over time (from 0000 GMT to 0600 GMT). This informs on relatively limited shear-driven vertical mixing of the surface layer momentum with the cloud region (Lothon et al., 2008; Knippertz et al., 2011). Notwithstanding, the nighttime LLC base was lowered by about 50 m between the two periods; which supports the observation of nocturnal cooling. There is a greater probability of cold air being advected over the area, which triggered most of the formation and maintenance of the LLC (see Figure 12). Again, there is likelihood of enhancements of the cold air advection by NLLJ. After all, in the IOP cases examined, significant cooling was observed, particularly, beneath the NLLJ core.

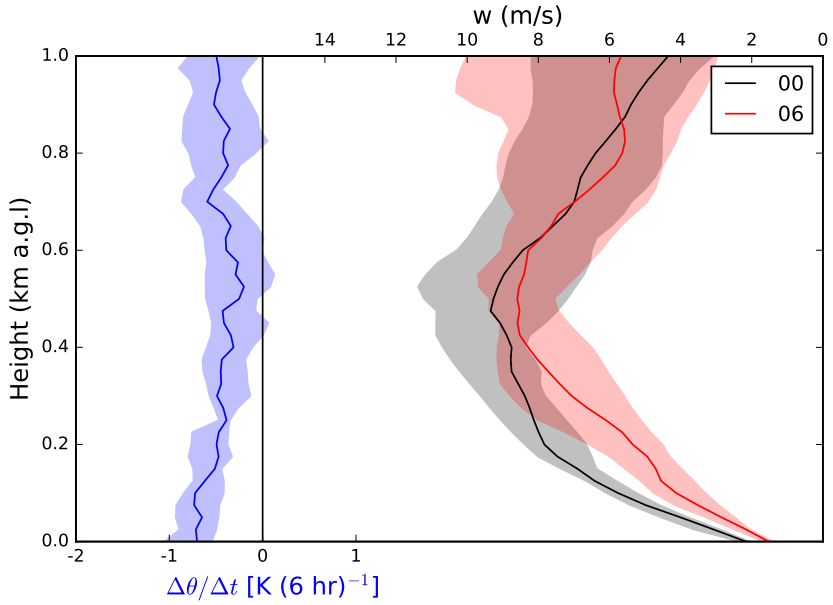

Figure 12. Net potential temperature change between 0000 GMT and 0600 GMT (blue) and wind speeds at 0000 GMT (black) and 0600 GMT (red). Continuous lines denote the median and filled area represents the 25^{th} and 75^{th} percentiles. The black vertical line marks separation of cooling (-) from warming (+).

Observations from Figure 12 support the argument by providing information on the net potential temperature change ($\Delta\theta/\Delta t$) between the hours of 0000 GMT and 0600 GMT, from the IOP radiosoundings. The radiosoundings of IOPs 5, 7, 11 and 12 were omitted from the analysis of net potential temperature change due to unavailability of one of the two radiosounding profiles. Significant cooling (negative net potential temperature change) is observed within the lowest kilometer, which is consistent with the recent findings of Adler et al. (2019) in Savè. This cooling is linked with the Gulf of Guinea maritime inflow (GoGMI): horizontal cold air advection related to the south-westerly Monsoon flow which transports maritime air from the Gulf of Guinea northwards over SWA (Adler et al., 2017, 2019; Deetz et al., 2018). GoGMI has been observed about several tens of kilometers from the coast, and initiated between the late afternoon and early evening. These propagate inland to distances beyond 100 km (Adler et al., 2017; Deetz et al., 2018).

5 Conclusion

With LLC being dominant in the West African domain and persistent till the following day, it has the tendency to impact on the radiative balance and regional climate, although its processes are not fully understood. This paper, as first step to understanding LLC development, validated ceilometer-deduced LLCs with the rather sparse, but *in situ*, radiosonde-deduced LLCs. Correlations of 0.68 was found between both procedures at 99 % significance level; revealing more than half of LLCs matched.

Thereafter, the aerosol backscatter from the ceilometer was used to assess the LLC evolution, its characteristic phases and how each individual phase of LLC development relates to the surface stability and surface energy balance. Observations made from this study were the formation of LLCs mostly between 2200 GMT and 2230 GMT, lasting throughout the night and positioned approximately few hundred meters, just below the NLLJ. Nocturnal cooling within the study region, thus lowers the LLC base between 0000 GMT and 0600 GMT and equally cools the PBL. Within this period, the surface is also stable to near-neutral, possibly influencing the dominance of neutral PBLs in Kumasi.

Thermal onsets at sunrise hour triggers transition from stable to unstable phase, which is marked by turbulence within the boundary layer, inducing mixing of atmospheric properties (eg. heat, momentum) within the layer. The accummulation and redistribution of heat within the lower layer tends to warm the lower atmosphere, triggering the rise of the LLC base, which eventually breaks up at approximately 0900 GMT from stratus cloud layers to more fragmented cloud layers. Between 1100 GMT and 1200 GMT, LLCs tend to dissipate; with some fraction ascending to higher altitudes.

Also, composites of the diurnal evolution of LLCs and their relationship with R_N, $\frac{dS}{dt}$ and ζ were assessed. It was evident that the dominance of LLCs at nighttime and their persistence long into the day have significant impact on R_N, by reducing $SW_{\downarrow}$. Additionally, onsets of LLCs were characterized by a near-steady state in the net radiation flux, whereas the rate of energy storage within the lower layers marginally oscillated about equilibrium.

On the formation of LLCs, the dominant factor identified from the study is horizontal cold air advection which seem to be enhanced by the NLLJ. The nocturnal cold air advection lowered the base of LLCs and cooled the boundary layer. Also, intermittently-turbulent structures were detected in the lower layers, beneath the NLLJ. However, these statically unstable regions were topped by statically stable regions which limited the influence of the unstable regions on the LLCs. Hence, for the observation period, contributions from shear-generated vertical mixing of moisture beneath the NLLJs were only marginal.

The findings of this paper are necessary for improving the understanding of low-level cloud characteristics, their formation and interactions with surface properties, particularly over

southern West Africa. The findings are again useful for improving the performance of PBL-based models over SWA, precisely their representation of LLC development.

Appendix A Background Atmospheric Profile

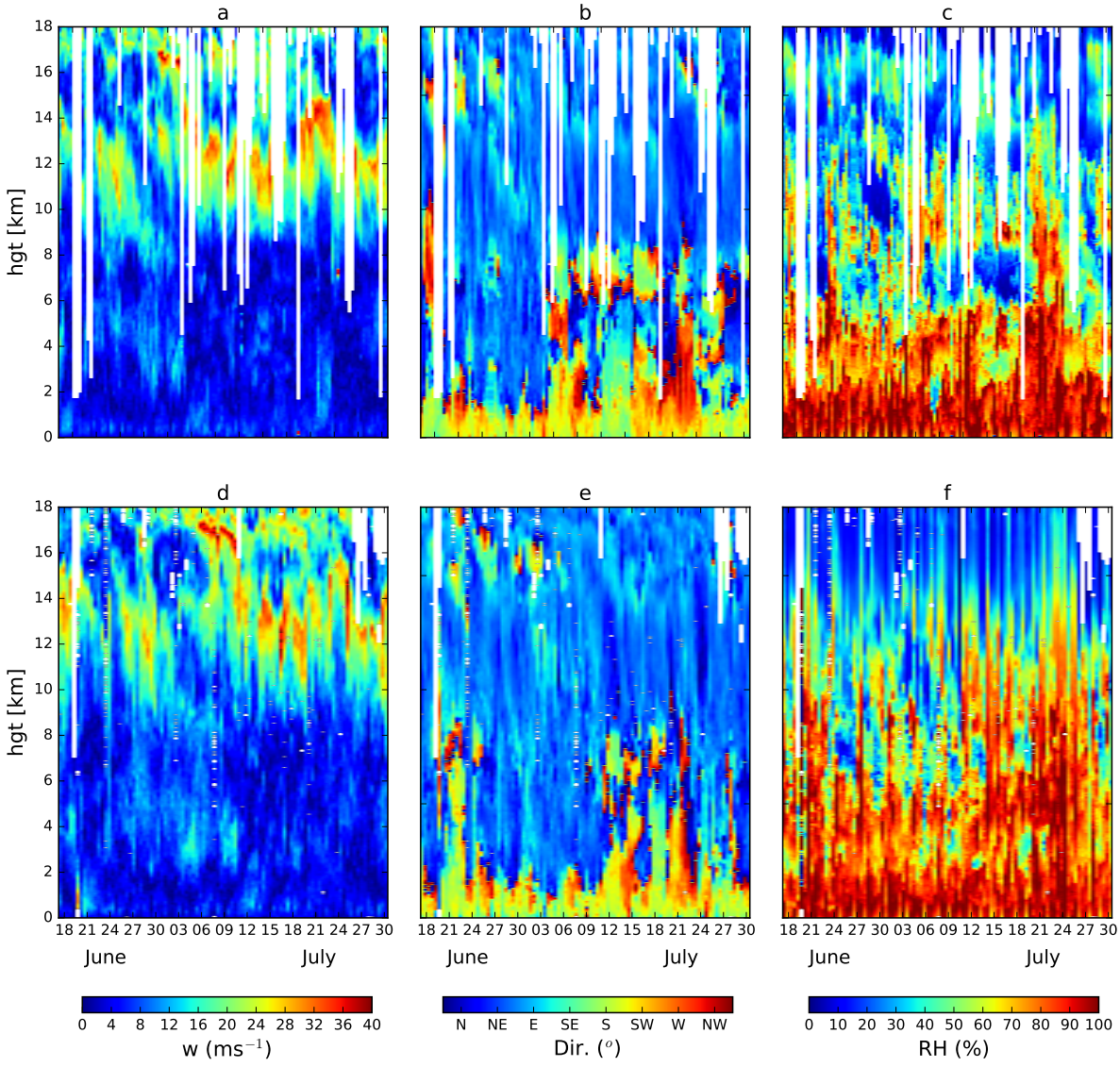

Figure A1. Upper air (wind speed:left, wind direction:middle and relative humidity:right) overview during the DACCIWA field campaign retrieved from radiosonde from the two supersites (Kumasi: above and Savè:below). Emphasis is laid on the above panel in this study.

Appendix B Ceilometer – Radiosonde LLC Validation and Diurnal Profiles of Selected IOP Variables

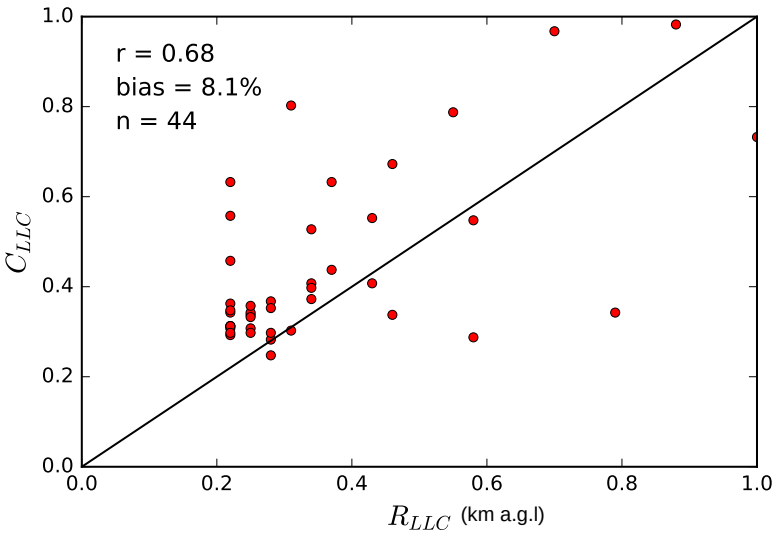

Figure B1. Validation of ceilometer LLCs with Radiosonde LLCs.

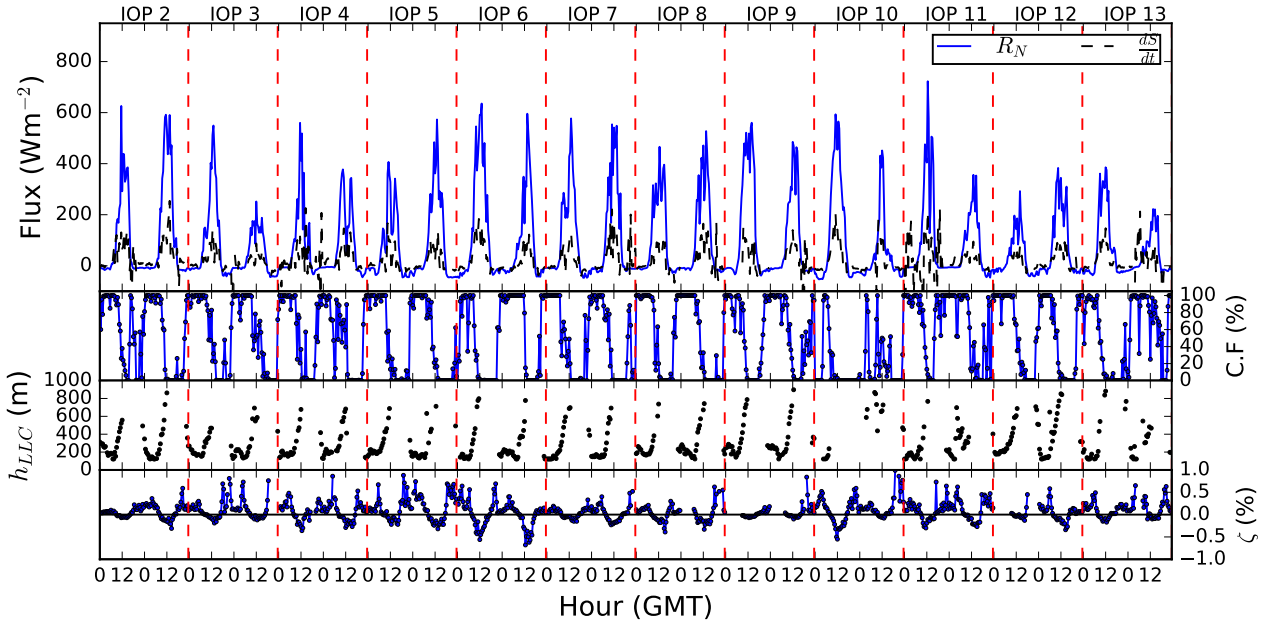

Figure B2. Diurnal profiles of energy flux, cloud fraction, LLC base height and surface stability during IOPs 2 – 13. Profiles are shown from 1-day pre-IOP to IOP day.

Acknowledgments

The research leading to these results has received funding from the European Union 7th Framework Programme (FP7/2007-2013) under Grant Agreement no. 603502 (EU project DACCIWA: Dynamics-aerosol-chemistry-cloud interactions in West Africa). The authors also acknowledge all collaborating institutions and personnel on the DACCIWA project, whose immense contribution during the 2016 DACCIWA Field Campaign, helped to gather relevant data for this study. Again, the authors are grateful to the Physics Department, KNUST for provision of workspace and other resources. The authors are again grateful to the anonymous reviewers for their comments and reviews that helped improve the paper. Data used in this study are accessible from http://baobab.sedoo.fr/DACCIWA/

Conflict of Interest

The authors declare no conflict of interest.

References

Adler, B., Babić, K., Kalthoff, N., Lohou, F., Lothon, M., Dione, C., ... Andersen, H. (2019). Nocturnal low-level clouds in the atmospheric 5 boundary layer over southern west africa: an observation-based analysis of conditions and processes. *Atmos. Chem. Phys.*, *19*, 663-681. doi: https://doi.org/10.5194/acp-2018-775

Adler, B., Kalthoff, N., & Gantner, L. (2017). Nocturnal low-level clouds over southern West Africa analysed using high-resolution simulations. *Atmospheric Chemistry and Physics*, *17*(2), 899–910.

Aryee, J., Amekudzi, L., Atiah, W., Osei, M., & Agyapong, E. (2018). Overview of surface to near-surface atmospheric profiles over selected domain during the QWeCI project. *Meteorology and Atmospheric Physics*, 1–15.

Aryee, J., Amekudzi, L., Quansah, E., Klutse, N., Atiah, W., & Yorke, C. (2018). Development of high spatial resolution rainfall data for Ghana. *International Journal of Climatology*, *38*(3), 1201–1215.

Babić, K., Adler, B., Kalthoff, N., Andersen, H., Dione, C., Lohou, F., ... Pedruzo-Bagazgoitia, X. (2019). The observed diurnal cycle of nocturnal low-level stratus clouds over southern west africa: a case study. *Atmos. Chem. Phys.*, *19*, 1281-1299. doi: https://doi.org/10.5194/acp-19-1281-2019

Baidu, M., Amekudzi, L. K., Aryee, J. N. A., & Annor, T. (2017). Assessment of Long-Term Spatio-Temporal Rainfall Variability over Ghana using Wavelet Analysis. *Climate*, *5*(2), 30.

Bessardon, G., Brooks, B. J., Abiye, O., Adler, B., Ajao, A., Ajileye, O., ... Wieser, A. (2018). A dataset of the 2016 monsoon season meteorology in southern West Africa - an overview from the DACCIWA campaign. *Sci. Data, in review*.

Bianca, A., Karmen, B., Norbert, K., Fabienne, L., Marie, L., Cheikh, D., ... Hendrik, A. (2018). Nocturnal low-level clouds in the atmospheric boundary layer over southern west africa: an observation-based analysis of conditions and processes. *sumitted to Atmospheric Chemistry and Physics*.

Böing, S. J., Jonker, H. J., Siebesma, A. P., & Grabowski, W. W. (2012). Influence of the subcloud layer on the development of a deep convective ensemble. *Journal of the Atmospheric Sciences*, *69*(9), 2682–2698.

Deetz, K., Vogel, H., Knippertz, P., Adler, B., Taylor, J., Coe, H., ... others (2018). Numerical simulations of aerosol radiative effects and their impact on clouds and atmospheric dynamics over southern West Africa. *Atmospheric Chemistry & Physics*, *18*(13).

Dione, C., Lohou, F., Lothon, M., Adler, B., Babić, K., Kalthoff, N., ... Gabella, O. (2018). Low level cloud and dynamical features within the south-

ern west african monsoon. *Atmos. Chem. Phys. Discuss.*, 1–33. doi: https://doi.org/10.5194/acp-2018-1149,2018

Flamant, C., Knippertz, P., Fink, A. H., Akpo, A., Brooks, B., Chiu, C. J., ... others (2017). The Dynamics-Aerosol-Chemistry-Cloud Interactions in West Africa field campaign: Overview and research highlights. *Bulletin of the American Meteorological Society*(2017).

Grabowski, W., Bechtold, P., Cheng, A., Forbes, R., Halliwell, C., Khairoutdinov, M., ... others (2006). Daytime convective development over land: A model intercomparison based on lba observations. *Quarterly Journal of the Royal Meteorological Society*, *132*(615), 317–344.

Grabowski, W. W. (2006). Indirect impact of atmospheric aerosols in idealized simulations of convective–radiative quasi equilibrium. *Journal of climate*, *19*(18), 4664–4682.

Hannak, L., Knippertz, P., Fink, A. H., Kniffka, A., & Pante, G. (2017). Why Do Global Climate Models Struggle to Represent Low-Level Clouds in the West African Summer Monsoon? *Journal of Climate*, *30*(5), 1665–1687.

Kalthoff, N., Lohou, F., Brooks, B., Jegede, G., Adler, B., Babić, K., ... others (2018). An overview of the diurnal cycle of the atmospheric boundary layer during the West African monsoon season: results from the 2016 observational campaign. *Atmospheric Chemistry and Physics*, *18*(4), 2913–2928.

Knippertz, P., Coe, H., Chiu, J. C., Evans, M. J., Fink, A. H., Kalthoff, N., ... others (2015). The DACCIWA project: Dynamics–aerosol–chemistry–cloud interactions in West Africa. *Bulletin of the American Meteorological Society*, *96*(9), 1451–1460.

Knippertz, P., Fink, A. H., Deroubaix, A., Morris, E., Tocquer, F., Evans, M. J., ... others (2017). A meteorological and chemical overview of the DACCIWA field campaign in West Africa in June-July 2016. *Atmospheric Chemistry and Physics*, *17*(17), 10893–10918.

Knippertz, P., Fink, A. H., Schuster, R., Trentmann, J., Schrage, J. M., & Yorke, C. (2011). Ultra-low clouds over the southern West African monsoon region. *Geophysical research letters*, *38*(21).

Lothon, M., Saïd, F., Lohou, F., & Campistron, B. (2008). Observation of the diurnal cycle in the low troposphere of west africa. *Monthly Weather Review*, *136*(9), 3477–3500.

Madougou, S., Saïd, F., Campistron, B., Lothon, M., & Kebe, C. (2012). Results of UHF radar observation of the nocturnal low-level jet for wind energy applications. *Acta Geophysica*, *60*(5), 1413–1453.

Pawlowska, H., Grabowski, W. W., & Brenguier, J.-L. (2006). Observations of the width of cloud droplet spectra in stratocumulus. *Geophysical Research Letters*, *33*(19).

Schepanski, K., Knippertz, P., Fiedler, S., Timouk, F., & Demarty, J. (2015). The sensitivity of nocturnal low-level jets and near-surface winds over the sahel to model resolution, initial conditions and boundary-layer set-up. *Quarterly Journal of the Royal Meteorological Society*, *141*(689), 1442–1456.

Schrage, J. M., & Fink, A. H. (2012). Nocturnal continental low-level stratus over tropical West Africa: Observations and possible mechanisms controlling its onset. *Monthly Weather Review*, *140*(6), 1794–1809.

Schuster, R., Fink, A. H., & Knippertz, P. (2013). Formation and maintenance of nocturnal low-level stratus over the southern West African monsoon region during AMMA 2006. *Journal of the Atmospheric Sciences*, *70*(8), 2337–2355.

Turner, D. D., Vogelmann, A., Austin, R. T., Barnard, J. C., Cady-Pereira, K., Chiu, J. C., ... others (2007). Thin liquid water clouds: Their importance and our challenge. *Bulletin of the American Meteorological Society*, *88*(2), 177–190.

van der Linden, R., Fink, A. H., & Redl, R. (2015). Satellite-based climatology

of low-level continental clouds in southern West Africa during the summer monsoon season. *J. Geophys. Res. Atmos.*, *120*, 11861201.

Wang, J., & Rossow, W. B. (1995). Determination of cloud vertical structure from upper-air observations. *J. Appl. Meteorol.*, *34*(10), 2243–2258. doi: 10.1175/1520-0450(1995)034⟨2243:DOCVSF⟩2.0.CO;2